



HAL
open science

Essential requirement for zebrafish anosmin-1a in the migration of the posterior lateral line primordium.

Constantin Yanicostas, Sylvain Ernest, Cyrielle Dayraud, Christine Petit, Nadia Soussi-Yanicostas

► **To cite this version:**

Constantin Yanicostas, Sylvain Ernest, Cyrielle Dayraud, Christine Petit, Nadia Soussi-Yanicostas. Essential requirement for zebrafish anosmin-1a in the migration of the posterior lateral line primordium.. *Developmental Biology*, 2008, 320 (2), pp.469-79. 10.1016/j.ydbio.2008.06.008 . inserm-00289099

HAL Id: inserm-00289099

<https://inserm.hal.science/inserm-00289099>

Submitted on 2 Jul 2008

HAL is a multi-disciplinary open access archive for the deposit and dissemination of scientific research documents, whether they are published or not. The documents may come from teaching and research institutions in France or abroad, or from public or private research centers.

L'archive ouverte pluridisciplinaire **HAL**, est destinée au dépôt et à la diffusion de documents scientifiques de niveau recherche, publiés ou non, émanant des établissements d'enseignement et de recherche français ou étrangers, des laboratoires publics ou privés.

Article accepted for publication in *Developmental Biology* : 3 Jun 2008

**Requirement for zebrafish anosmin-1a in the migration of the posterior
lateral line primordium**

Yanicostas Constantin^{1,*}, Ernest Sylvain^{2,*}, Dayraud Cyrielle¹, Petit Christine³ and
Soussi-Yanicostas Nadia¹

¹*INSERM Equipe Avenir, IFR Neurosciences (IFR 70) Hôpital de la Pitié-Salpêtrière,
47 Bd de l'Hôpital, 75651 Paris, France.*

²*INSERM, U368, 46 rue d'Ulm, 75230 PARIS, France.*

³*INSERM, U587, Institut Pasteur, 25 rue du Dr Roux, 75015 Paris, France.*

Correspondence should be addressed to:

Dr. Nadia Soussi-Yanicostas

INSERM Equipe Avenir, Pavillon de l'enfant et de l'adolescent

CHU Pitié-Salpêtrière, 47 Bd de l'Hôpital - 75651 Paris cedex 13

Tel 33(0)142162676

E-mail : soussi@chups.jussieu.fr

Key words: Anosmin-1, Kallmann syndrome, *Kal1a* gene, Zebrafish, Cell migration,
Lateral line primordium, SDF1a.

*These authors contributed equally to this work

Abstract

Kallmann syndrome (KS) is a human genetic disease that impairs both cell migration and axon elongation. The *KAL-1* gene underlying the X-linked form of KS, encodes an extracellular matrix protein, anosmin-1, which mediates cell adhesion and axon growth and guidance *in vitro*. We investigated the requirement for *kal1a* and *kal1b*, the two orthologues of the *KAL-1* gene in zebrafish, in the journey of the posterior lateral line primordium (PLL). First, we established that while the accumulation of *kal1a* and *kal1b* transcripts was restricted to the posterior region of the migrating primordium and newly deposited neuromasts, the encoded proteins, anosmin-1a and anosmin-1b, respectively, were accumulated in the PLL, in differentiated neuromasts and in a thin strip extending along the trail path of the PLL. We also show that morpholino knockdown of *kal1a*, but not *kal1b*, severely impairs PLL migration. However, while the PLL of *kal1a* morphants displays highly abnormal morphology, proper expression of the *cxcr4b* gene suggests that *kal1a* does not play a role in PLL differentiation. Conversely, wild-type levels of *kal1a* transcripts are detected in the PLL of *cxcr4b*, *sdf1a* or *sdf1b* morphant embryos, strongly suggesting that *kal1a* transcription is independent of CXCR4b/SDF1a signalling. Last, moderate depletion of both anosmin-1a and SDF1a markedly affects PLL migration providing strong evidence that anosmin-1a acts as an essential co-factor in SDF1a-mediated signalling pathways. Our findings, which demonstrate, for the first time, an essential requirement for anosmin-1a in PLL migration, also strongly suggest that this protein plays a key role for proper activation of the CXCR4b/SDF1a and/or CXCR7/SDF1a signalling pathway in PLL migration.

Introduction

Genetic neurological disorders offer a powerful approach to identify proteins involved in the setting up of neural networks. They thus provide further insight into the molecular processes underlying axon growth and guidance and neuron migration. Kallmann syndrome (KS) (Kallmann et al., 1944; de Morsier, 1955) is a human genetic disease that impairs cell migration and axon elongation. In KS patients, both the elongation of olfactory neuron axons and the migration of gonadotropin-releasing hormone (GnRH) synthesizing neurons, are defective (Schwanzel-Fukuda et al., 1989). The *KAL-1* gene, underlying the X-linked form of the disease (Franco et al. 1991; Legouis et al. 1991), encodes a cell matrix protein, anosmin-1, that displays cell adhesion, neurite outgrowth, axon guidance and axon branch-promoting activities *in vitro* (Soussi-Yanicostas et al., 1996; 1998; 2002; Rugarli et al., 1996; Hardelin et al., 1999; Robertson et al., 2001). Cariboni et al. (2004) have also demonstrated that anosmin-1 affects the migration of GnRH neurons *in vitro* and we have established that it also modulates the migratory properties of a glial cell population *in vitro*, namely the oligodendrocyte precursors in the developing optic nerve in rodents (Bribian et al., 2006).

In zebrafish, two *KAL-1* orthologues, namely *kal1a* and *kal1b* (Ardouin et al., 2000), encoding anosmin-1a and anosmin-1b, respectively, have been identified. Whitlock et al. (2005) and Okubo et al. (2006) have demonstrated an essential requirement for anosmin-1a, but not for anosmin-1b, in GnRH cell migration in zebrafish and medaka, respectively. In addition, while *kal1a* and *kal1b* display distinct patterns of transcription during zebrafish development, both genes are expressed to high levels in another migrating cell population, the PLLP (Ardouin et al., 2000). The lateral line (LL) is a mechanosensory organ of fish and amphibians that senses water movements and thus helps fish to avoid obstacles and predators, detect prey, and swim in groups. In fish, the LL comprises several rows of small, discrete and evenly spaced sensory organs, the neuromasts, which contain some ten sensory hair cells each. The posterior LL (PLL), the main branch of which derives from the migration of the PLLP, comprises the neuromasts located on the flanks and tail of fish. In the zebrafish, the PLLP originates from a sensory placode that forms just caudal to the otic vesicle at about 18 hours post-fertilization (hpf) (Kimmel et al., 1995) and begins to migrate along the myoseptum toward the tail at around 20 hpf (for reviews, see Dambly-Chaudière et al., 2003; Ghysen and Dambly-Chaudière, 2004; 2007; Lecaudey and Gilmour, 2006). At regular intervals throughout its journey, small groups of cells located at the trailing edge of the PLLP progressively

slow down and then stop to split off from the migrating primordium. These groups of cells, the proneuromasts, will eventually differentiate into neuromasts. During its travel, the PLLP evenly deposits 5 neuromasts along the flanks of the fish and 2 to 3 neuromasts clustered in the tail region. By 42 hpf, PLLP migration is achieved and 6 hours later all the neuromasts are fully differentiated (Gompel et al., 2001; Ledent, 2002). Neuromasts are innervated by bipolar sensory neurons that also differentiate from the PLL placode. These neurons are clustered into two cranial ganglions and send out two axons each, one into the hindbrain and the second into the PLLP (Metcalf et al., 1985). Evidence suggests that their growth cones contact the cells of the PLLP before the beginning of migration and remain associated with these cells throughout their journey (Metcalf, 1985). Previous studies have identified the chemokine receptors CXCR4b and CXCR7 and their ligand SDF-1a as the components of a signalling pathway that plays a key role in PLLP migration (David et al., 2002; Li et al., 2004; Sapède et al., 2005; Haas et al., 2006; Dambly-Chaudière et al., 2007; Valentin et al., 2007).

We demonstrated an essential requirement for anosmin-1a, but not for anosmin-1b, in PLLP migration. We found that while the differentiation of the PLLP was not impaired in *kal1a* morphant, its journey was severely compromised following morpholino-mediated *kal1a* inactivation. We also showed that *kal1a* transcription is independent of CXCR4b/SDF1a signalling. Last, we observed that moderate depletion of both anosmin-1a and SDF1a markedly affects PLLP migration, strongly suggesting that anosmin-1a is an essential co-factor in SDF1a-mediated signalling.

Materials and methods

Zebrafish Strains

Zebrafish (*Danio rerio*) were maintained as described by Westerfield (1995). Embryos were produced in our facility using standard conditions. Wild-type embryos were from the AB strain. Transgenic animals from the *H₂A.F/Z::GFP* and *ClaudinB::GFP* transgenic lines were kindly provided by J. Campos-Ortega (Pauls et al., 2001) and D. Gilmour (Haas et al., 2006), respectively.

DASPEI labelling

Hair cells were labelled by incubating 5 dpf living embryos in DASPEI solution (100 µg/ml in fish water) for 10 min at room temperature. Embryos were quickly rinsed in fish water, oriented in methylcellulose (3% in fish water), imaged using a 5 X objective mounted on a Leica DMRBE microscope equipped with a Nikon digital Sight DS-U1 camera and the stained neuromasts were counted unilaterally.

Antibody production

Two rabbit polyclonal antibodies raised against zebrafish anosmin-1a (Genbank AF163310) have been generated: α anosmin1a-A and α anosmin1a-B, which are directed against peptides corresponding to N-terminal residues 151 to 197 and C-terminal residues 1051 to 1096, respectively. We have also generated two rabbit polyclonal antibodies directed against anosmin-1b (Genbank AF163311): α anosmin1b-A and α anosmin1b-B, which are directed against peptides including N-terminal residues 51 to 102 and C-terminal residues 851 to 899, respectively.

All antibodies were affinity purified and their specificity was verified by Western blots. Substitution of the purified anti-anosmin-1a or anti-anosmin-1b antibodies by the pre-immune sera and pre-adsorption of the antibodies with the corresponding antigens were used as negative controls.

Western blotting

Zebrafish protein extracts were analyzed by immunoblotting as described by Gershoni and Palade (1983). Anti-anosmin-1a-A and anosmin-1b-A were used at a 1:1,000 dilution. Horseradish peroxidase (HRP)-conjugated anti-rabbit antibody was

used as secondary antibodies at a 1:6000 dilution, and chemiluminescence was detected using the ECL kit (Amersham).

Morpholino-mediated gene Inactivation

To inactivate the translation of *kal1a* RNAs, we designed a morpholino-oligonucleotide, MO *kal1a* (5'-GGTGAGCCCGTCTCGCATCTTGAAG-3'), which is complementary to the sequence flanking on the both sides the translation initiating codon of the *kal1a* RNA (underlined). Similarly, we designed a morpholino aimed at inhibiting the translation of *kal1b* RNAs, MO *kal1b* (5'-GCAGAGATTCCTCAAAGCAGCATC-3'). As control, we first designed a morpholino oligonucleotide derived from MO *kal1a* but comprising five mismatching bases (lower case letters), mmMO *kal1a*, (5'-GGTcAGgCCGTgTCGCATgTTcAAG-3'). We also used a non-specific morpholino oligonucleotide, MO control (5'-CCTCTTACCTCAGTTACAATTTATA-3'). To inactivate the translation of *cxcr4b* and *sdf1a* RNAs, C. Dambly-Chaudière and A. Ghysen kindly provided us with MO *cxcr4b* (5'-ATGATGCTATCGTAAAATTCCATTT-3') and MO *sdf1a* (5'-ATCACTTTGAGATCCATGTTTGCA-3'). For morpholino-mediated transcript inactivation experiments, solutions 0.1, 0.25 or 0.5 mM of the different morpholinos were injected using standard protocols. For double inactivation of *kal1a* and *kal1b* transcripts, a mix of MO *kal1a* and MO *kal1b*, 0.25 mM each, was injected. For double inactivation of *kal1a* and *sdf1a* RNAs, a mix of MO *kal1a* and MO *sdf1a*, 0.1 mM each, was injected.

Production of a kal1a morpholino-insensitive kal1a RNA

To synthesize MO *kal1a*-insensitive *kal1a* transcripts, the complete translated sequence of a *kal1a* cDNA was subcloned as XhoI-XbaI fragment in the pCS2+ plasmid. A mutated version of *kal1a* protein coding sequence was obtained by PCR using a forward oligonucleotide complementary to the *kal1a* DNA sequence flanking the ATG codon and including 7 mis-matches mutations (lower case letters): 5' cTCgAGATGCGcGAtGGaCTtACTGGTTTG 3' and containing a Xho I restriction site (5' to the ATG), and a reverse oligonucleotide that binds 3' to the termination codon and containing a Xba I restriction site (note that all mutations do not change the amino acid sequence of anosmin-1a). The PCR product was then cloned as Xho I-Xba I fragment in the pCS2+ plasmid to generate the pCS2+/*kal1a* construct. This plasmid was linearized by Not I digestion and then used as templates for *in vitro*

transcription. MO *kal1a*-insensitive *kal1a* RNA was generated using the SP6 mMESSAGE mMACHINE kit (AMBION) following the protocol provided by the manufacturer.

Phenotypic rescue

For rescue experiments, a mix containing MO *kal1a* (0,5 mM) and MO *kal1a*-insensitive *kal1a* mRNA (1 μ M), was injected into embryos at the one- to two-cell stage according to standard protocols and the phenotypes were analysed at the indicated stages.

Whole-mount in situ hybridization

In situ hybridization was performed as described in R&D Systems kit (R&D Systems Europe, Lille, France). The following cDNA were used as templates to synthesize riboprobes: *kal1a* (Ardouin et al., 2000; Genbank AF163310), *kal1b* (Ardouin et al., 2000; Genbank AF163311), *cxcr4b* (ZFIN NM_131834; Chong et al., 2001; Gompel et al., 2001; David et al., 2002), *sdf1* (ZFIN NM_178307; Chong et al., 2001; Gompel et al., 2001; David et al., 2002) and *tacstd* (ZFIN NM_213175; Villabianca et al., 2006).

Immunofluorescence on whole mount embryos

Embryos were fixed in 4% formaldehyde in PBS for 1h at room temperature, washed three times in PBS (10 mn each) and incubated overnight at 4°C with the anti-anosmin-1a or anti-anosmin-1b antibodies diluted 1:1000 or anti-acetylated β -tubulin antibodies diluted 1:200 in PBS containing 1% bovine serum albumin. Following incubation with primary antibodies, embryos were incubated with Alexa 488-conjugated goat anti-rabbit Fab'2 antibodies diluted 1:500 in PBS supplemented with 1% BSA for 1h at room temperature, washed as previously described and oriented in methylcellulose (3% in fish water).

PLL nerve labelling and time-lapse microscopy

In vivo imaging of posterior lateral line primordium (PLL) migration was performed in *H₂A.F/Z::GFP* transgenic (WT) (Pauls et al., 2001), MO *kal1a*-injected

H₂A.F/Z::GFP, *ClaudinB::GFP* transgenic (WT) (Haas et al., 2006), and *MO kal1a*-injected *ClaudinB::GFP* embryos. *In vivo* imaging of PLLP migration in *H₂A.F/Z::GFP* transgenic embryos, was recorded for 90 minutes, approximately, by time-lapse confocal microscopy of embryos aged from 32 to 33.5 hpf. *In vivo* imaging of PLLP migration in *Claudin::B::GFP* transgenic embryos, was recorded for 60 minutes, approximately, by time-lapse apotome microscopy of embryos aged from 26 to 27 hpf. LL sensory neurons and the PLLP nerve were labelled by Dil injection into the PLLP ganglion. Images were acquired on a Zeiss LSM confocal microscope and an Apotome Zeiss microscope.

Statistics

Statistical analysis was performed using one-way ANOVA.

RESULTS

Kal1a and kal1b are transcribed in the migrating cells of the PLLP

The PLLP forms just caudal to the otic vesicle at 18 hpf and at 20 hpf starts migrating toward the caudal region to reach the tip of the tail by 40 hpf (for reviews, see Dambly-Chaudière et al., 2003; Ghysen and Dambly-Chaudière, 2004; 2007; Lecaudey and Gilmour, 2006). First, we re-examined the pattern of transcription of the two orthologues of the *KAL-1* gene in zebrafish, *kal1a* and *kal1b*, throughout PLLP migration in embryos aged from 22 to 38 hpf. In close agreement with previous results (Ardouin et al., 2000), *kal1a* and *kal1b* transcription was observed first in the newly differentiated PLLP at approximately 20 hpf (data not shown) and high levels of both transcripts were detected in the migrating PLLP throughout its journey toward the tip of the tail (Fig. 1A-I). Within the migrating primordium, up to 28 hpf approximately, *kal1a* and *kal1b* are predominantly transcribed in the posterior region of the PLLP comprising the migrating cells with *kal1a*, and more especially *kal1b* expression, decreasing sharply to become barely detectable in the cells located within the trailing region of the primordium, which soon stops migrating to differentiate into neuromasts (Fig. 1J and K). However, from 28 hpf onward approximately, contrasting with previous results (Ardouin et al., 2000), high levels of *kal1a* transcription were also detected in newly deposited neuromasts and to a lesser extent, in differentiated neuromasts (supplementary Fig. 1A-D).

Distribution of anosmin-1a and anosmin-1b during PLL differentiation

We then studied the distribution of anosmin-1a and anosmin-1b throughout PLLP migration using specific antibodies (see Materials and methods). The distribution of the two proteins does not precisely fit that of the corresponding RNAs. At 20 hpf, in close agreement with *in situ* hybridization data, both proteins were present in the newly differentiated PLLP (data not shown). From 26 hpf onward, anosmin-1a and anosmin-1b accumulated in the centre of the trailing region of the PLLP and, in close agreement with our previous data (Ernest et al., 2007), from 32 hpf onward, both proteins were detected in differentiated neuromasts (Fig. 1L-O). Anosmin-1a and anosmin-1b were also distributed along the myoseptum as a discontinuous thin strip extending along the trailing path of the migrating primordium (Fig. 1L and O). In the head region, anosmin-1a was found in the anterior lateral line primordium (ALLP) and head neuromast hair cells (supplementary Fig. 2A-B”).

Kal1a inactivation impairs neuromast deposition

We used morpholino-mediated gene knock-down to study the consequences of *kal1a* and *kal1b* transcript-inactivation on PLL differentiation. First, we used Western blot to show that injection of MO *kal1a* or MO *kal1b* inhibited translation of the corresponding mRNAs. In wild-type embryos, anti-anosmin-1a or anti-anosmin-1b antibodies each revealed a single band of approximately 95 kDa (Fig. 2H and I, lanes 1). In embryos injected with a 5 bp-mismatched *kal1a* morpholino, [mmMO *kal1a* (0.5 mM)] (Fig. 2H, lane 2) or with a standard control morpholino (Fig. 2I, lane 2), the same proteins were detected. In contrast, *kal1a* morphants [(MO *kal1a* (0.5 mM) and (0.1 mM)] showed a complete absence of anosmin-1a or strongly reduced levels of the protein, respectively (Fig. 2H, lanes 3 and 4). Similarly, anosmin-1b was undetectable in protein extracts from *kal1b* morphant [MO *kal1b* (0.5 mM)] (Fig. 2I, lane 3). These data thus demonstrate the efficiency of the morpholinos used in this study.

First, we analysed the differentiation of the PLL in *kal1a* and *kal1b* morphants by counting the number of neuromasts deposited along the flanks and tail of embryos at 3 dpf using the fluorescent vital dye DASPEI (Whitfield et al., 1996) (Fig. 2A-F). Non-injected embryos (WT) and embryos injected with mmMO *kal1a* (0.5 mM) displayed 7.37 ± 0.26 ($n = 150$) and 6.17 ± 0.42 ($n = 120$) neuromasts per side, respectively (Fig. 2A and D). Morpholino-mediated *kal1a* inactivation induced a sharp decrease in the number of deposited neuromasts, with embryos injected with *kal1a* MO *kal1a* (0.25 mM) or (0.5 mM), showing 2.15 ± 0.52 ($n = 132$, $p < 0.05$) and 0.69 ± 0.15 ($n = 250$, $p < 0.01$ vs. WT and mmMO *kal1a*) neuromasts per side, respectively (Fig. 2B and C). By contrast, *kal1b* inactivation did not affect the differentiation of the PLL, with *kal1b* morphants [MO *kal1b* (0.5 mM)] displaying 7.50 ± 0.26 ($n = 95$, $p < 0.01$ vs. WT) neuromasts per side. To verify that the reduced number of neuromasts observed in *kal1a* morphants was not due to a non-specific effect of the morpholino used in this study, we tested whether co-injection of a *kal1a* MO-insensitive *kal1a* RNA was able to rescue the neuromast deposition defect observed in *kal1a* morphants. The results show that in embryos co-injected with MO *kal1a* (0.5 mM) and *kal1a* MO-insensitive *kal1a* RNA (1 μ M), the number of deposited neuromasts, 6.15 ± 0.45 ($n = 96$) (Fig. 2F), was not significantly different from that observed in wild-type embryos ($p < 0.05$) or mmMO *kal1a* morphants ($p < 0.01$). In addition, at 4, 5, and 8 dpf, while the number of deposited neuromasts

was on average similar in wild-type and *kal1b* morphants, their numbers were reduced by 93 to 100% and 92 to 100% in *kal1a* morphants, compared with wild-type or MO *kal1b*-injected embryos, respectively ($p < 0.01$; Fig. 2G). These results demonstrate that the absence of neuromasts in *kal1a* morphants was not the consequence of a delayed differentiation of proneuromasts into neuromasts. Moreover, comparative analysis of the pigmentation pattern together with eye and mouth differentiation in MO *kal1a* (0.5 mM) morphants aged between 3 and 5 dpf show that embryonic development, and consequently LL differentiation, were not significantly delayed in anosmin-1a-depleted embryos compared with wild-type embryos (supplementary Fig. 3A-D'). To ascertain that the reduced number of neuromasts observed in *kal1a* morphants was not the mere consequence of the absence of hair cells, we combined DASPEI staining with transgenic *ClaudinB:GFP* embryos as recipients for morpholino injection. Results show that in MO *kal1a* (0.25 mM) morphants, almost all deposited neuromasts display hair cells (Fig. 2J-K'') and support cells (Fig. 2L, M) as evidenced by *in situ* detection of *tacstd* transcripts (Villabianca et al., 2006). However, in these morphant embryos the number of hair cells per neuromast was reduced (6.4 ± 2.4 hair cells/neuromast; $n=17$) when compared to wild-type embryos (11.1 ± 0.8 hair cells/neuromast; $n=13$) and the regular "rosette"-like organization of these cells was altered (Fig. 2J-K''). In good agreement with anosmin-1a accumulation in neuromast hair cells (Ernest et al., 2007 and Fig. 2J-K''), these data suggest that anosmin-1a also plays a role in terminal differentiation of these cells. The lack of neuromasts in strong MO *kal1a* (0.5 mM) morphants was confirmed independently using scanning electron microscopy (data not shown). By contrast, both morpholino-mediated loss-of-function and RNA injection-mediated over-expression experiments show that *kal1b* does not play an essential role in PLL differentiation. Therefore, we did not investigate the function of this gene any further here.

We also observed that the formation of the anterior LL was affected, though at milder levels, following *kal1a* inactivation. In embryos injected with MO *kal1a* (0.25 mM) or (0.5 mM) a reduction of approximately 50 and 80%, respectively, of the number of cephalic neuromasts was observed compared with wild-type embryos (Fig. 2A-C).

Essential requirement for anosmin-1a in PLLP migration

The lack of PLL neuromasts in *kal1a* morphants may be the consequence of the failure of several developmental processes: (i) PLLP differentiation, (ii) correct

migration of the PLLP along the body axis, and/or (iii) the deposition of proneuromasts from the migrating primordium. To address these issues and determine whether the PLLP properly differentiate and (or) migrate in *kal1a* morphants, these embryos were analysed first at 28 hpf by *in situ* hybridization using a *cxcr4b* probe, which strongly labels the PLLP throughout its migration (David et al., 2002). In wild-type (Fig. 3A) and mmMO *kal1a* (0.5 mM) embryos (Fig. 3C), a strong labelling of the PLLP was observed throughout its journey toward the tip of the tail. High levels of *cxcr4b* transcripts were also detected in the PLLP of *kal1a* morphants. However, in these embryos, *cxcr4b* staining revealed that PLLP migration was severely abrogated (Fig. 3B). These findings strongly suggest that *kal1a* inactivation does not inhibit PLLP differentiation, but markedly compromises its migration.

To further assess the specificity of MO *kal1a*-mediated gene inactivation, embryos were injected with *kal1a* MO-insensitive *kal1a* RNA (1 μ M) alone or co-injected with MO *kal1a* (0.5 mM) and *kal1a* MO-insensitive *kal1a* RNA (1 μ M), and then hybridized with a *cxcr4b* probe. *Cxcr4b* staining revealed that the PLLP was located at a similar position along the body axis in wild-type embryos compared with those injected with *kal1a* MO-insensitive *kal1a* RNA (compare Fig. 3A with D), showing that injection of the modified *in vitro* transcribed *kal1a* RNA did not affect PLLP migration. Similarly, results showed that PLLP migration was not impaired in embryos co-injected with MO *kal1a* and *kal1a* MO-insensitive *kal1a* RNA when compared with wild-type embryos or those injected with the *kal1a* MO-insensitive *kal1a* RNA alone (compare Fig. 3E with 3A and D). These data demonstrate that exogenously supplied anosmin-1a is able to fully overcome the lack of the endogenous protein and thus the specificity of the effect of MO *kal1a*-mediated gene inactivation on PLLP migration.

To investigate the consequences of *kal1a* inactivation on the morphology of the PLLP, we used *ClaudinB::GFP* embryos as recipients for MO *kal1a* injection. These embryos display an intense fluorescent labelling of all derivatives of sensory placodes, including the PLLP (Haas et al., 2006) (Fig. 4A and A'). In close agreement with *cxcr4b* staining, results confirm that PLLP migration was severely impaired in *ClaudinB::GFP* MO *kal1a* morphants (0.5 mM) ($n=51$) (Fig. 4B-C'). In addition, while the PLLP displayed a stretched morphology in non-injected embryos (Fig. 4A'), the PLLP of *ClaudinB::GFP* *kal1a* morphants showed abnormal morphologies, being either rounded ($n=48$) (Fig. 4B') or C-shaped ($n=3$) (Fig. 4C').

Kal1a inactivation induces a severe freeze of PLLP migration

While our data show that migration of the PLLP is severely impaired in *kal1a* morphants, we cannot rule out the possibility that the journey of the PLLP is not frozen but only severely slowed. To establish whether *kal1a* inactivation impairs PLLP migration or only severely reduces its speed, we followed primordium migration *in vivo* by time-lapse analysis using *H2A.F/Z::GFP* (Pauls et al., 2001) and *ClaudinB::GFP* transgenic embryos (Haas et al., 2006) as recipients for MO *kal1a* (0.5 mM) injection. In addition, we injected the fluorescent vital dye Dil in the PLLP ganglion at 22 hpf to visualize PLLP sensory neurons and their axons, and thus follow the location of the PLLP nerve respectively to the migrating primordium. In close agreement with earlier observations (Metcalf, 1985; Gompel et al., 2001), *in vivo* imaging revealed that in wild-type embryos, the PLLP migrated at a speed of approximately 1.5 somites per hour (Fig. 5A, C, C' and C'' and supplementary Movies 1 and 3). In contrast, the PLLP and its associated nerve were immobilized in MO *kal1a* (0.5 mM) morphants, thus confirming that *kal1a* inactivation severely impairs PLLP migration (Fig. 5B, D, D' and D'' and supplementary Movies 2 and 4). However, in MO *kal1a* (0.25 mM) morphants, while the PLLP nerve migrated up to the trailing region of the PLLP, its nerve fibres did not extend within the primordium (supplementary Fig. 4). These data demonstrate that while *kal1a* inactivation does not block the elongation of the PLLP nerve, it impairs the full extension of sensory neuron axons within the migrating PLLP.

Transcription of kal1a in the migrating PLLP is independent of CXCR4b/SDF-1 signalling

It has been shown that *cxcr4b*, which encodes a chemokine receptor, and one of its ligands, SDF1a, play key roles during PLLP migration in zebrafish embryos (David et al., 2002; Li et al., 2004; Sapède et al., 2005; Haas et al., 2006). In the migrating PLLP, *cxcr4b* transcription is detected in the posterior half of the primordium that contains migrating cells, and is down-regulated in the cells of the trailing region (Gompel et al., 2001), as is also the case for the *kal1a* gene. The co-expression of the two genes in the migrating cells of the PLLP suggests that the CXCR4b receptor may positively regulate *kal1a* transcription.

To test this hypothesis, we investigated by *in situ* hybridization whether *kal1a* transcription was down-regulated following morpholino-mediated inactivation of the *cxcr4b* or *sdf1a* genes. As previously described, in the absence of SDF1a or CXCR4b, the migration of the PLLP is blocked (David et al., 2002; Li et al., 2004;

Sapède et al., 2005; Haas et al., 2006; Dambly-Chaudière et al., 2007; Valentin et al., 2007). However, the expression of the *kal1a* gene in the PLLP, notwithstanding its location along the body axis, was not significantly altered in *cxcr4b* (Fig. 6B) or *sdf1a* (Fig. 6C) morphants compared with wild-type embryos (Fig. 6A). Thus transcription of the *kal1a* gene in the migrating PLLP is independent of the CXCR4b/SDF1a signalling pathway.

Moderate depletion of both anosmin-1a and SDF1a markedly affects PLLP migration

While *kal1a* transcription in PLLP cells is independent of CXCR4b/SDF1a signalling, co-expression of the *kal1a* and *cxcr4b* or *cxcr7* genes in PLLP cells, also suggests that the cell matrix protein anosmin-1a may be a cofactor of CXCR4b or CXCR7 in SDF1a-mediated signalling.

To test this hypothesis, we investigated by morpholino injections whether moderate depletion of both anosmin-1a and SDF1a compromises PLLP migration. Interestingly, results show that while the journey of the PLLP was not significantly impaired in MO *sdf1a* (0.1 mM) ($n=32$) (Fig. 7B) and MO *kal1a* (0.1 mM) ($n=73$) (Fig. 7C) morphants, embryos co-injected with MO *kal1a* and MO *sdf1a* (0.1 mM each) ($n=41$) display severe PLLP migration defects (Fig. 7D-D''), reminiscent to those observed in strong MO *kal1a* (0.5 mM) morphants (compare Fig. 7D'' with Fig. 4B'), thus strengthening the hypothesis that anosmin-1a is an essential co-factor in SDF1a-mediated signalling.

DISCUSSION

We demonstrate here an essential requirement for the zebrafish *kal1a* gene in PLLP migration. We had previously shown that in the inner ear and in differentiated neuromasts, anosmin-1a is accumulated at the surface of hair cells, suggesting a hitherto unknown function for this protein in mechanosensory cells (Ernest et al., 2007). Thus our findings provide strong evidence that anosmin-1a plays different roles during the differentiation of the PLL. In particular, our results suggest that anosmin-1a is an essential co-factor in SDF1a/CXCR4b and/or SDF1a/CXCR7 signalling pathways.

Anosmin-1a plays an essential role during PLLP migration

The severe PLLP migration defect observed in *kal1a* morphants, which can be rescued by co-injecting a morpholino-insensitive *kal1a* RNA, provides strong evidence that anosmin-1a plays an essential role during the journey of the PLLP. In addition, both the specific transcription of *kal1a* and the accumulation of anosmin-1a in the migrating PLLP suggest a direct requirement for this protein in the migratory properties of PLLP cells.

Anosmin-1 is an ECM protein also required for the migration of another cell population, the GnRH synthesizing neurons. In close agreement with the migration defect of GnRH cells observed in Kallmann's patients (Schwandzel-Fukuda et al., 1989), previous works have established that anosmin-1a plays an essential and evolutionarily conserved role during the migration of GnRH neurons from the olfactory placode to the brain in both zebrafish (Whitlock et al., 2005) and medaka (Okubo et al., 2006). In these cases, while the *kal1a* gene is not expressed in the migrating GnRH neurons (Okubo et al., 2005), it is transcribed in the olfactory bulbs, which are a step point along the migration path of these neurons during their journey to the hypothalamus. In addition, *in vitro* experiments in mammals have shown that exogenously supplied anosmin-1 displays a specific chemotactic activity on immortalized mouse GnRH neurons (GN11) (Cariboni et al., 2004).

We have also demonstrated that zebrafish anosmin-1a, like human anosmin-1 (Soussi-Yanicostas et al., 1996; 1998; Robertson et al., 2001), is a secreted protein and an ECM component that displays several activities *in vitro*, including axon growth and guidance and, of particular interest here, cell adhesion (Soussi-Yanicostas, unpublished data). In addition, two mutations that abolish the chemotactic activity of anosmin-1 on GnRH (GN11) neurons (Cariboni et al., 2004) also affect the cell

adhesion properties of the protein (Robertson et al., 2001), suggesting a possible direct link between these two activities. Overall, these data suggest that during GnRH neuron migration, anosmin-1/anosmin-1a acts non-autonomously and plays a role as a guidance cue and (or) migration substrate.

By contrast, during the journey of the PLLP, both the accumulation of anosmin-1a in the PLLP from approximately 20 hpf onward, just before the onset of migration, and the phenotypes of the PLLP of *kal1a* morphants, suggest that the PLLP migration defect is the result of a cell autonomous defect affecting PLLP cells, which inhibits their ability to move. In particular, the severe migration defect observed following partial depletion of both anosmin-1a and SDF1a, provides strong evidence that anosmin-1a plays an essential role for proper activation of SDF1a-mediated signalling in PLLP cells expressing CXCR4b and/or CXCR7. This hypothesis is also reinforced by the rounded phenotype of the PLLP observed in approximately 94% of *kal1a* morphants (48/51), which is reminiscent of that observed in *cxcr4b* mutants (Hass et al., 2006). Also, the C-shaped phenotype of the PLLP observed in approximately 5% of *kal1a* morphants, suggests that following *kal1a* inactivation, part of the PLLP cells may be attracted by the ventral expression domain of SDF1a located at the level of the pronephros (David et al., 2002). Altogether, these data strongly suggest an essential requirement for anosmin-1a in SDF1a/CXCR4b and/or SDF1a/CXCR7 signalling.

Given the results of *in vitro* studies, which have demonstrated that anosmin-1 binds directly to urokinase-type plasminogen activator and activates its amidolytic activity (Hu et al., 2004), an attractive hypothesis would be that anosmin-1/anosmin-1a acts as a scaffold protein that recruits proteases and locally increases the proteolytic degradation of extracellular matrix components, and thus the release or activation of growth factors or receptor ligands, including SDF1a.

Multiple requirements for anosmin-1a in lateral line differentiation

Transcription of the *kal1a* gene is detected first in the newly differentiated PLLP at approximately 20 hpf and throughout its migration, *kal1a* RNAs are specifically expressed in the posterior region of the primordium that contains the migrating PLLP cells. In addition, from 36 hpf onward, *kal1a* transcript accumulation is also observed in the newly deposited neuromasts. In contrast, throughout the journey of the PLLP, anosmin-1a accumulation is detected in the centre of the anterior region, along the trailing path of the primordium and, in close agreement with our previous results (Ernest et al., 2007), in differentiated neuromast hair cells. This accumulation pattern

combined with the reduced number and disorganization of the neuromast hair cells observed in intermediate MO *kal1a* (0.25 mM) morphants suggest that anosmin-1a may be also required for proper hair cell differentiation. However, we cannot rule out the possibility that the disorganization of the few neuromasts deposited in intermediate MO *kal1a* (0.25 mM) morphants is the mere consequence of the PLLP migration defect observed in these embryos.

In addition, the accumulation of anosmin-1a along a thin discontinuous strip extending along the trailing path of the migrating primordium also suggests that a secreted form of anosmin-1a is deposited by the cells of the migrating primordium at the surface of underlying mesodermal cells. This hypothesis is supported by previous data showing that human anosmin-1 is a secreted protein (Soussi-Yanicostas et al., 1996; Rugarli et al., 1996). An interesting possibility is that this deposited form of anosmin-1a might play a role in the full maturation of the adjacent PLL nerve, such as the guidance of glial cells along sensory neuron axons or proper myelination of the nerve fibres. In this context, it is interesting to note that while the LL nerve elongates up to the trailing edge of the PLLP whatever its position along the A-P axis in intermediate MO *kal1a* (0.25 mM) morphants, its axons do not properly defasciculate nor enter the primordium, suggesting a possible role for anosmin-1a in terminal elongation of the LL nerve or proper innervation of the PLLP.

Anosmin-1b is dispensable for PLLP migration and neuromasts deposition

Intriguingly, while both *kal1a* and *kal1b* RNAs are transcribed in the PLLP throughout its journey, the analysis of *kal1b* morphants and *kal1a-kal1b* double-morphants strongly suggests that anosmin-1b is fully dispensable for PLLP migration. As mentioned above, Whitlock et al. (2005) and Okubo et al. (2006) have shown that the *kal1a/kal1.1*, but not *kal1b/kal1.2*, genes play an essential role during the migration of GnRH cells in zebrafish and medaka, respectively. Also, an enlargement of the body cavity of embryos has been observed following antisense peptide nucleic acid (PNA)-mediated *kal1.1* inactivation (Okubo et al., 2006). However, none of these defects are observed following MO *kal1b*-mediated gene inactivation (Whitlock et al., 2005 and our results), the efficiency of which was confirmed by Western blot, and no abnormalities were detected following inactivation of the *kal1.2* RNAs (Okubo et al. 2006). Given the levels of sequence similarities between the zebrafish *kal1a* and *kal1b* and the medaka *kal1.1* and *kal1.2* genes, Okubo et al. (2006) have proposed that *kal1.1* and *kal1.2* are the orthologues of *kal1a* and *kal1b*, respectively. In this context, it is interesting to note that: (i)

anosmin-1b lacks the basic C-terminal domain found in all vertebrate anosmin-1 so far characterized, (ii) its N-terminal cysteine-rich region contains amino acid substitutions that affect two cysteine residues, which are conserved in all other vertebrate anosmin-1 and (iii) its WAP motif also displays three amino acid substitutions that affect residues that are conserved in all vertebrate anosmin-1 (supplementary Fig. 6). The lack of detectable phenotypes in embryos following *kal1b/kal1.2* inactivation combined with the absence of the basic C-terminal domain in this protein and the amino acid substitutions described above, raise questions about the function of the *kal1b/kal1.2* genes. However, given its structure and sequence, it is very unlikely that *kal1b* is a pseudogene. Also, this gene, which arose from a gene duplication predating the divergence of teleosts and tetrapods (Okubo et al., 2006), is conserved in both the medaka and zebrafish. Taken together, these data suggest that anosmin-1b plays a role in processes that remain to be discovered.

Our data identify the ECM protein anosmin-1a as an essential factor for PLLP migration, suggesting an evolutionarily conserved function for this protein in cell migration processes. In addition, while several lines of evidence strongly suggest that anosmin-1 is a partner of FGF Receptor 1 in mammals, the present data provide functional evidence *in vivo* strongly suggesting that anosmin-1a is an essential co-factor of SDF1a in PLLP migration. This last result is an important advance in the field, which paves the way to better understanding the molecular processes underlying the requirement for anosmin-1a in SDF1a-mediated signalling and works in this direction are currently in progress. These investigations should also improve our knowledge of the role of extracellular matrix/ligand/receptor interactions during PLLP migration and also provide us with a better understanding of the physiopathology of the X-linked form of KS.

Legends to figures

Fig. 1. Transcription of the *kal1a* and *kal1b* genes and accumulation of anosmin-1a and anosmin-1b, throughout PLLP migration. *In situ* detection of *kal1a* (**A-F** and **J**) and *kal1b* (**G-I** and **K**) transcripts in 22 to 38 hpf whole-mount embryos. Magnified views of the primordium at 32 hpf (**J** and **K**). The direction of migration is from anterior to posterior. Whole-mount immunodetection of anosmin-1a (**L-M**) and anosmin-1b (**N-O**) in 30 hpf embryos. Magnified views of the embryos shown in **L** (**M**) and **N** (**O**). Prim: PLLP; L2: neuromast 2; pL2, pL3: pro-neuromasts 2 and 3. neu: differentiated neuromasts.

Fig. 2. Morpholino-induced *kal1a*, but not *kal1b*, inactivation impairs PLL neuromast deposition as visualized by DASPEI staining. Wild-type (WT) embryo (**A**), MO *kal1a* (0.25 mM) (**B**) or (0.5 mM) (**C**), mmMO *kal1a* (0.5 mM) (**D**), MO *kal1b* (0.5 mM) morphants (**E**) and MO *kal1a* (0.5 mM) morphant co-injected with MO *kal1a*-insensitive *kal1a* RNA (1 μ M) (**F**). Time course of neuromast deposition in WT embryos ($n=48$), *kal1a* (0.5 mM) ($n=53$) and *kal1b* (0.5 mM) morphants ($n=45$) from 3 to 8 dpf (**G**). Values are means \pm s.e.m. Western blot analysis of anosmin-1a accumulation (**H**) in 3 dpf WT embryos (**1**), mmMO *kal1a* (0.5 mM) (**2**), MO *kal1a* (0.5 mM) (**3**) and (0.1 mM) morphants (**4**) and anosmin-1b accumulation (**I**) in 3 dpf WT embryos (**1**), MO control (**2**) and MO *kal1b* (0.5 mM) morphants (**3**). L1-L6: neuromasts lined up along the flanks of embryos; ter: neuromasts clustered in the tail region. Neuromast organization in intermediate MO *kal1a* (0.25 mM) morphant (**K-K'** and **M**) and wild-type embryos (**J-J'** and **L**) visualized by DASPEI staining of hair cells on *ClaudinB::GFP* embryos (**J-K'**) and *in situ* detection of *tacstd* transcripts in neuromast support cells (**L**, **M**). Arrows indicate neuromasts. n: neuromast.

Fig. 3. Migration of the PLLP is defective following inactivation of the *kal1a*, but not *kal1b*, gene as visualized by whole-mount *in situ* detection of *cxcr4b* RNAs at 28 hpf. Wild-type (WT) embryo (**A**), MO *kal1a* (0.5 mM) (**B**) and mmMO *kal1a* morphants (0.5 mM) (**C**), embryo injected with MO *kal1a*-insensitive *kal1a* RNA (1 μ M) alone (**D**) and MO *kal1a* (0.5 mM) morphant injected with MO *kal1a*-insensitive *kal1a* RNA (1 μ M) (**E**). Arrows indicate the leading edge of the migrating PLLP.

Fig. 4. *Kal1a* inactivation affects the morphology of the PLLP. 28 hpf *ClaudinB::GFP* embryo (**A** and **A'**) and *ClaudinB::GFP* embryos injected with MO *kal1a* (0.5 mM) (**B** to **C'**). Magnified views of the primordium of the embryos shown in

A (A'), **B (B')** and **C (C')**. Arrows indicate the PLLP. e: ear. Scale bar= 200 μm in (**A**, **C**), 100 μm in (**B**) and 50 μm in (**A'**, **B'**, **C'**).

Fig. 5. *Kal1a* inactivation severely compromises PLLP migration as shown by Dil labelling of the axon of PLL sensory neurons in *H2A.F/Z::GFP* (**A** and **B**) and *ClaudinB::GFP* (**C** to **D''**) embryos. *In vivo* imaging of PLLP migration by time-lapse confocal microscopy from 32 to 33.5 hpf in a *H2A.F/Z::GFP* embryo (**A**) and a *H2A.F/Z::GFP* MO *kal1a* (0,5 mM) morphant (**B**), and apotome microscopy from 26 to 27 hpf in a *ClaudinB::GFP* embryo (**C** to **C''**) and a *ClaudinB::GFP* MO *kal1a* (0,5 mM) morphant (**D** to **D''**) following Dil injection into the PLLP ganglion. Dashed lines: PLLP leading edge; n: recently deposited neuromast. PLLg: posterior lateral line ganglion, e: ear, WT: wild type. Arrows indicate the tip of the PLLP nerve. Anterior-posterior axis is from left to right.

Fig. 6. *Kal1a* transcription in the PLLP is independent of CXCR4b/SDF1a signalling. *In situ* detection of *kal1a* transcripts on whole-mount 28 hpf wild type embryo (**A**) and *cxcr4b* (**B**) and *sdf1a* morphants (**C**). Arrows indicate the PLLP.

Fig. 7. Moderate depletion of both anosmin-1a and SDF1a markedly affects PLLP migration. 26 hpf *ClaudinB::GFP* embryo (**A**) and *ClaudinB::GFP* embryos injected with MO *sdf1a* (0,1 mM) (**B**), MO *kal1a* (0.1 mM) (**C**) or co-injected with a mix of MO *sdf1a* and MO *kal1a* (0.1 mM each) (**D**). Magnified views the primordium of the embryo shown in **D** (**D'** and **D''**). Arrows indicate the PLLP. e: ear. Scale bar= 200 μm in (**A-C**), 300 μm in (**B**), 100 μm in (**D'**) and 50 μm in (**D''**).

Legends to supplementary figures

Fig. S1. Pattern of *kal1a* transcript accumulation in primordia of 26 (A, C) and 33 hpf (B, D) whole-mount embryos. Magnified views of the primordium of the embryos shown in A (C) and B (D). Arrows (A and B) and dashed lines (C and D) indicate the leading edge of primordia. Prim: primordium.

Fig. S2. Localisation of anosmin-1a in the anterior lateral line primordium (ALLP) and head neuromast hair cells. Pattern of accumulation of anosmin-1a (A'-A'') in the head region (A-D) and head neuromast hair cells (C, D) of 26 hpf *ClaudinB::GFP* embryos. Merge image of the photographs shown in A and A' (A''). White arrows indicate the ALLP. e: ear; v: vitellus; n: neuromast; ALLP: anterior lateral line primordium.

Fig. S3. Embryonic development is not delayed following *kal1a* inactivation. Pigmentation pattern and morphology of 3 (A-B') and 4 dpf (C-D') wild-type embryos (A, A', C and C') and MO *kal-1a* (0.5 mM) morphants (B, B', D and D'). Magnified views of the head of the embryos shown in A (A'), B (B'), C (C') and D (D'). Arrows indicate the mouth.

Fig. S4. *Kal1a* inactivation compromises terminal elongation of the PLLP nerve within the migrating primordium. Dil labelling of the axon of PLL sensory neurons in control *H2A.F/Z::GFP* embryos (A) and following injection of MO *kal1a* (0.25 mM) (B) and (0.5 mM) (C). Dashed lines: PLLP leading edge.

Fig. S5. *Kal1a* inactivation compromises terminal elongation of the PLLP nerve within the migrating primordium. Acetylated β -tubulin immunostaining of the PLLP nerve (A', B', C' and D') in *ClaudinB::GFP* embryos (A, B) and following injection of MO *kal1a* (0.5 mM) (C, D). Magnified views of the primordium shown in A (B), A' (B'), A'' (B''), C (D), C' (D') and C'' (D''). Merge images of the photographs shown in A and A' (A''), B and B' (B''), C and C' (C'') and D and D' (D''). Arrows indicate the distal edge of the PLLP nerve. v: vitellus, e: ear.

Fig. S6. Comparison of the structure and sequence of anosmin-1 and of its different domains in vertebrate and invertebrate species. Structure of zebrafish anosmin-1a and -1b and human anosmin-1 (a). Amino acid substitutions in the anosmin-1b N-terminal domain, of residues, which are conserved between human

anosmin-1 and zebrafish anosmin-1a (**b**). Comparison of the peptidic sequences of the cysteine-rich region (C-box) (**c**), Whey acidic protein (WAP) motif (**d**), heparan sulphate (HS) binding site (**e**) and histidine (His) rich C-terminal domain (**f**) of anosmin-1 in various vertebrate and invertebrate species. FnIII: fibronectin type III repeat; H: Homo; D. rerio: Danio rerio; P: Pan, B. taurus: Bovis taurus; C. familiaris: Canis familiaris; G: Gallus; C. japonica: Carassius japonica; X: Xenopus; F: Fugu; T: Tetraodon; A. gambiae: Anopheles gambiae; A. mellifera: Apis mellifera; B. mori: Bombyx mori; C. elegans: Caenorhabditis elegans; C. briggsae: Caenorhabditis briggsae; D. melanogaster: Drosophila melanogaster. The cysteine residues of the C box and the amino acids of the WAP motif consensus sequence are boxed in dark blue; the PEK motif of the WAP motif that is conserved in vertebrate is boxed in light blue; the aspartate or glutamate residues found in vertebrate anosmin-1 WAP motif are boxed in dark green; the basic residues of the heparan sulphate binding site and of the histidine-rich and basic region are boxed in light green; the amino acid substitutions specific of anosmin-1b are boxed in red.

Movie 1. PLLP migration as shown by Dil labelling of the axon of PLL sensory neurons in a *H2A.F/Z::GFP* embryo. *In vivo* imaging by time-lapse confocal microscopy of PLLP migration from 32 to 33.5 hpf, in a *H2A.F/Z::GFP* embryo following Dil injection into the PLLP ganglion. Dashed line: PLLP leading edge; n: recently deposited neuromast. Anterio-posterior axis is from left to right.

Movie 2. *Kal1a* inactivation freezes PLLP migration as shown by Dil labelling of the axon of PLL sensory neurons in *H2A.F/Z::GFP* embryos. *In vivo* imaging by time-lapse confocal microscopy of PLLP migration from 32 to 33.5 hpf, in a *H2A.F/Z::GFP* embryo following MO *kal1a*- (0,5 mM) mediated *kal1a* gene inactivation and Dil injection into the PLLP ganglion. Dashed line: PLLP leading edge; n: recently deposited neuromast. Anterio-posterior axis is from left to right.

Movie 3. PLLP migration as shown by GFP staining and Dil labelling of the axon of PLL sensory neurons in a *ClaudinB::GFP* embryo. *In vivo* imaging by time-lapse apotome microscopy of PLLP migration from 26 to 27 hpf, in a *ClaudinB::GFP* embryo following Dil injection into the PLLP ganglion. Anterio-posterior axis is from left to right.

Movie 4. *Kal1a* inactivation freezes PLLP migration as shown by GFP staining and Dil labelling of the axon of PLL sensory neurons in *ClaudinB::GFP* embryos. *In*

vivo imaging by time-lapse apotome microscopy of PLLP migration from 26 to 27 hpf, in a *ClaudinB::GFP* embryo following MO *kal1a* (0,5 mM) -mediated *kal1a* gene inactivation and Dil injection into the PLLP ganglion. Anterio-posterior axis is from left to right.

Acknowledgements

We thank D. Gilmour for the gift of the *ClaudinB::GFP* transgenic line, J. Campos-Ortega for providing the *H2A.F/Z::GFP* transgenic line, B. and C. Thisse for the *cxcr4b* probe, C. Dambly-Chaudière and A. Ghysen for the gift of the *cxcr4b* and *sdf1a* morpholinos and Aurélie Dipietromari for her help with *in situ* hybridization. This work was supported by the INSERM Avenir program (No. R04190SP), the Fondation pour la Recherche Médicale (FRM No. INE20050303379), and the Fondation NRJ de l'Institut de France.

References

- Ardouin, O., Legouis, R., Fasano, L., David-Watine, B., Korn, H., Hardelin, J.-P., Petit, C., 2000. Characterization of the two zebrafish orthologues of the *KAL-1* gene underlying X chromosome-linked Kallmann syndrome. *Mech. Dev.* 90 98-94.
- Bribian, A., Barallobre, M.J., Soussi-Yanicostas, N., de Castro, F., 2006. Anosmin-1 modulates the FGF-2-dependent migration of oligodendrocyte precursors in the developing optic nerve. *Mol. Cell. Neurosci.* 33 2-14.
- Cariboni, A., Pimpinelli, F., Colamarino, S., Zaninetti, R., Piccolella, M., Rumio, C., Piva, F., Rugarli, E.I., Maggi, R., 2004. The product of X-linked Kallmann's syndrome gene (*KAL1*) affects the migratory activity of gonadotropin-releasing hormone(GnRH)-producing neurons. *Hum. Mol. Genet.* 13 2781-2791.
- Chong, S.W., Emelyanov, A., Gong, Z., Korzh, V., 2001. Expression pattern of two zebrafish genes, *cxcr4a* and *cxcr4b*. *Mech. Dev.* 109, 347-354.
- Dambly-Chaudière, C., Sapède, D., Soubiran, F., Decorde, K., Gompel, N., Ghysen, A., 2003. The lateral line of zebrafish: a model system for the analysis of morphogenesis and neural development in vertebrates. *Biol. Cell* 95, 579-587.
- Dambly-Chaudière, C., Cubedo, N., Ghysen, A., 2007. Control of cell migration in the development of the posterior lateral line: Antagonistic interactions between the chemokine receptors CXCR4 and CXCR7/RDC1. *BMC Dev. Biol.* 7(23), doi: 10.1186/1471-213X-7-23.
- David, N.B., Sapède, D., Saint-Etienne, L., Thisse, C., Thisse, B., Dambly-Chaudière, C., Rosa, F., Ghysen, A., 2002. Molecular basis of cell migration in the fish lateral line: Role of the chemokine receptor CXCR4 and of its ligand, SDF1. *Proc. Natl. Acad. Sci. U.S.A.* 99, 16297-16302.
- de Morsier, G., (1955). Etudes sur les dysraphies crânio-encéphaliques. 1. Agénésie des lobes olfactifs (telencephaloschizis lateral) et des commissures calleuse et antérieure (telencephaloschizis median). La dysplasie olfacto-génitale. *Schweiz. Arch. Neurol. Psychiat.* 74, 309-361.

- Ernest, S., Guadagnini, S., Prévost, M.-C., Soussi-Yanicostas, N., 2007. Localization of anosmin-1a and anosmin-1b in the inner ear and neuromasts of zebrafish. *Genes Expr. Patterns* 7, 274-281.
- Franco, B., Guioli, S., Pragliola, A., Incerti, B., Bardoni, B., Tonlorenzi, R., Carrozzo, R., Maestrini, E., Pieretti, M., Taillon-Miller, P., Brown, C.J., Willard, H.F., Lawrence, C., Persico, M.G., Camerino, G., Ballabio, A., 1991. A gene deleted in Kallmann's syndrome share homology with neural cell adhesion and axonal path-finding molecules. *Nature* 353, 529-536.
- Gershoni, J.M., Palade, G.E., 1983. Protein blotting: Principles and applications. *Anal Biochem.* 131, 1-15.
- Ghysen, A., Dambly-Chaudière, C., 2004. Development of the zebrafish lateral line. *Curr. Op. Neurobiol.* 14, 67-73.
- Ghysen, A., Dambly-Chaudière, C., 2005. The three-sided romance of the lateral line: glia love axons love precursors love glia. *BioEssay* 27, 488-494.
- Ghysen, A., Dambly-Chaudière, C. 2007. The lateral line microcosmos. *Genes Dev.* 21, 2118-2130.
- Gompel, N., Cubedo, N., Thisse, C., Thisse, B., Dambly-Chaudière, C., Ghysen, A., 2001. Pattern formation in the lateral line of zebrafish. *Mech. Dev.* 105, 69-77.
- Hardelin, J.-P., Julliard, A.K., Moniot, B., Soussi-Yanicostas, N., Verney, C., Schwandzel-Fukuda, M., Ayer-Le Lievre, C., Petit, C., 1999. Anosmin-1 is a regionally restricted component of basement membranes and interstitial matrices during organogenesis: implications for the developmental anomalies of X chromosome-linked Kallmann syndrome. *Dev. Dyn.* 215, 26-44.
- Haas, P., Gilmour, D., 2006. Chemokine signalling mediates self-organizing tissue migration in the zebrafish lateral line. *Dev. Cell* 10, 673-680.
- Hu, Y., González-Martinez, D., Kim, S.-H., Bouloux, P.M.G., 2004. Cross-talk of anosmin-1, the protein implicated in X-linked Kallmann's syndrome, with heparan sulphate and urokinase-type plasminogen activator. *Biochem. J.* 384, 495-505.

- Kallmann, F.J., Schoenfeld, W.A., Barrera, S.E., (1944). The genetic aspects of primary eunuchoidism. *Am. J. Mental Deficiency* 48, 203-236.
- Kimmel, C.B., Ballard, W.W., Kimmel, S.R., Ullmann, B., Schilling, T.F., 1995. Stages of embryonic development of the zebrafish. *Dev. Dyn.* 233, 253-310.
- Lecaudey, V., Gilmour, D., 2006. Organizing moving groups during morphogenesis. *Curr. Op. Cell Biol.* 18, 102-107.
- Ledent, V., 2002. Postembryonic development of the posterior lateral line in zebrafish. *Development*, 129, 597-604.
- Legouis, R., Hardelin, J.-P., Levillier, J., Claverie, J.-M., Compain, S., Wunderle, V., Millasseau, P., Le Paslier, D., Cohen, D., Carerina, D., Bougueleret, L., Delemarre-Van de Waal, H., Lutfalla, G., Weissenbach, J., Petit, C., 1991. The candidate gene for the X-linked Kallmann syndrome encodes a protein related to adhesion molecules. *Cell* 67, 423-435.
- Li, Q., Shirabe, K., Kuwada, J., 2004. Chemokine signaling regulates sensory cell migration in zebrafish. *Dev. Biol.* 269, 123-136.
- Metcalf, W.K., 1985. Sensory neuron growth cones comigrate with posterior lateral line primordium in zebrafish. *J. Comp. Neurol.* 238, 218-224.
- Okubo, K., Sakai, F., Lau, E.L., Yoshizaki, G., Takeuchi, Y., Naruse, K., Aida, K., Nagahama, Y., 2006. Forebrain gonadotropin-releasing hormone neuronal development: Insights from transgenic medaka and the relevance to X-linked Kallmann syndrome. *Endocrinology* 147, 1076-1084.
- Pauls, J., Geldmacher-Voss, B., Campos-Ortegas, J.A., 2001. A zebrafish histone variant H2A.F/Z and a H2A.F/Z:GFP fusion protein for in vivo studies of embryonic development. *Dev. Genes Evol.* 211, 603-610.
- Robertson, A., MacColl, G.S., Nash, J.A.B., Boehm, M.K., Perkins, S.J., Bouloux, P.-M.G., 2001. Molecular modelling and experimental studies of mutation and cell-adhesion sites in the fibronectin type III and whey acidic protein domains of human anosmin-1. *Biochem. J.* 357, 647-659.

- Rugarli, E.I., Ghezzi, C., Valsecchi, V., Ballabio, A., 1996. The Kallmann syndrome gene product expressed in COS cells is cleaved on the cell surface to yield a diffusible component. *Hum. Mol. Genet.* 5, 1109-1115.
- Sapède, D., Rossel, M., Dambly-Chaudière, C., Ghysen, A., 2005. Role of SDF1 chemokine in the development of lateral line efferent and facial motor neurons. *Proc. Natl. Acad. Sci. U.S.A.* 102, 1714-1718.
- Schwandzel-Fukuda, M., Bick, D., Pfaff, D.W., 1989. Luteinizing hormone-releasing hormone (LH-RH)-expressing cells do not migrate normally in an inherited hypogonadal (Kallmann) syndrome. *Molec. Brain Res.* 6, 311-326.
- Soussi-Yanicostas, N., Hardelin, J.-P., Arroyo-Jimenez, M., Ardouin, O., Legouis, R., Levilliers, J., Traincard, F., Betton, J.-M., Cabanié, L., Petit, C., 1996. Initial characterization of anosmin-1, a putative extracellular matrix protein synthesized by definite neuronal cell populations in the central nervous system. *J. Cell Sci.* 109, 1749-1757.
- Soussi-Yanicostas, N., Faivre-Sarrailh, C., Hardelin, J.-P., Levilliers, J., Rougon, G., Petit, C., 1998. Anosmin-1 underlying the X-chromosome linked Kallmann syndrome is an adhesive molecule that can modulate neurite growth in a cell-type specific manner. *J. Cell Sci.* 111, 2953-2965.
- Soussi-Yanicostas, N., de Castro, F., Julliard, A.K., Perfettini, I., Chédotal, A., Petit, C., 2002. Anosmin-1, defective in the X-linked form of Kallmann syndrome, promotes axonal branch formation from olfactory bulb output neurons. *Cell* 109, 217-228.
- Valentin, G., Haas, P., Gilmour, D., 2007. The chemokine SDF1a coordinates tissue migration through the spatially restricted activation of CxcR7 and CxcR4b. *Curr. Biol.* 17, 1026-1031.
- Villablanca, E.J., Renucci, A., Sapède, D., Lec, V., Soubiran, F., Sandoval, P.C., Dambly-Chaudière, C., Ghysen, A., Allende, M.L. 2006. Control of cell migration in the zebrafish lateral line: implication of the gene “tumour-associated calcium signal transducer”, *tacstd*. *Dev. Dyn.* 235, 1578-1588.
- Westerfield, M., 1995. *The Zebrafish Book* Univ. of Oregon, Eugene, OR.

Whitlock, K.E., Smith, K.M., Kim, H., Harden, M.V., 2005. A role for *foxd3* and *sox10* in the differentiation of gonadotropin-releasing hormone (GnRH) cells in the zebrafish *Danio rerio*. *Development* 132, 5491-5502.

Whitfield, T.T., Granato, M., van Eeden, F.J. Schach, U., Brand, M., Furutani-Seiki, M., Haffter, P., Hammerschmidt, M., Heisenberg, C.P., Jiang, Y.J., Kane, D.A., Kelsh, R.N., Mullins, M.C., Odenthal, J., Nüsslein-Volhard, C., 1996. Mutations affecting development of the zebrafish inner ear and lateral line. *Development*, 123, 241-254.

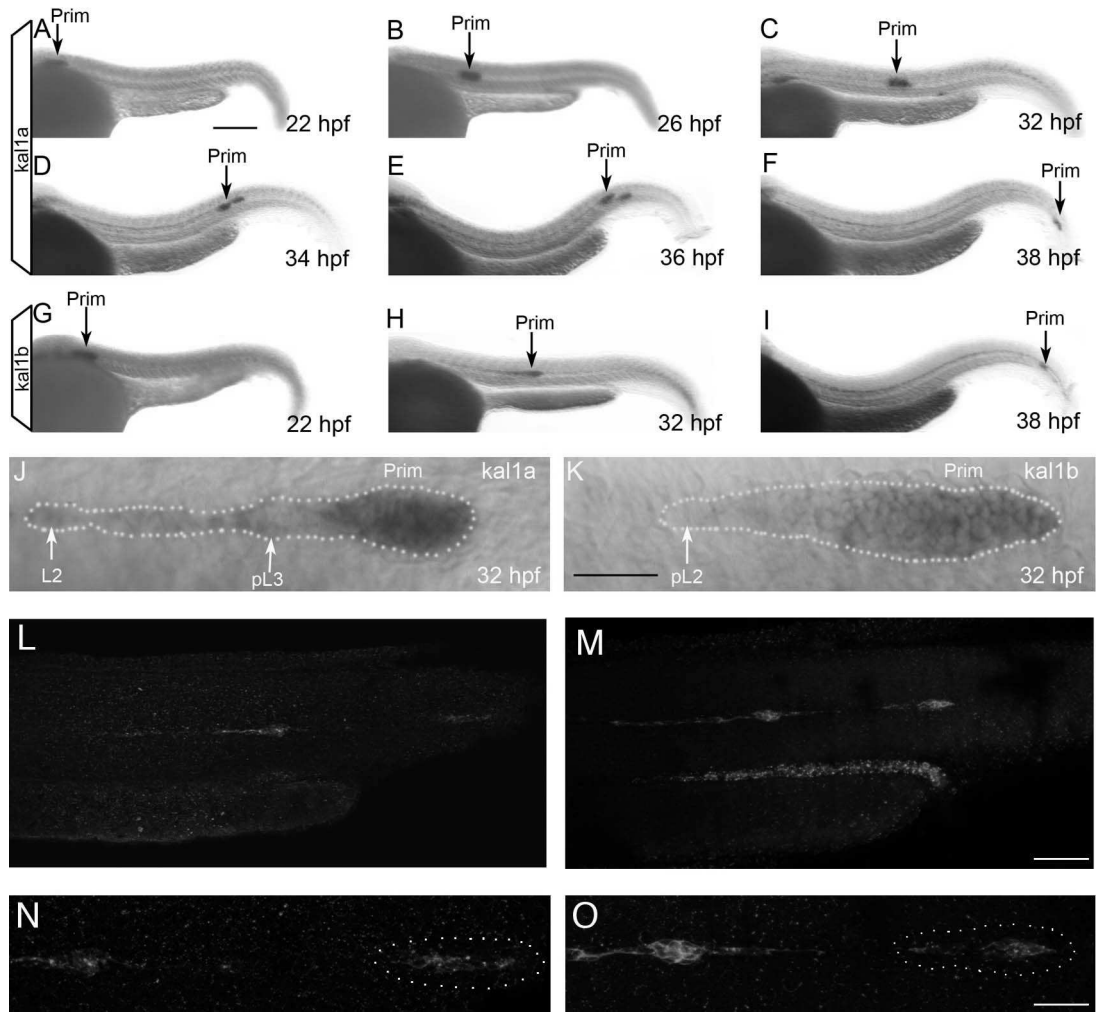


Figure 1

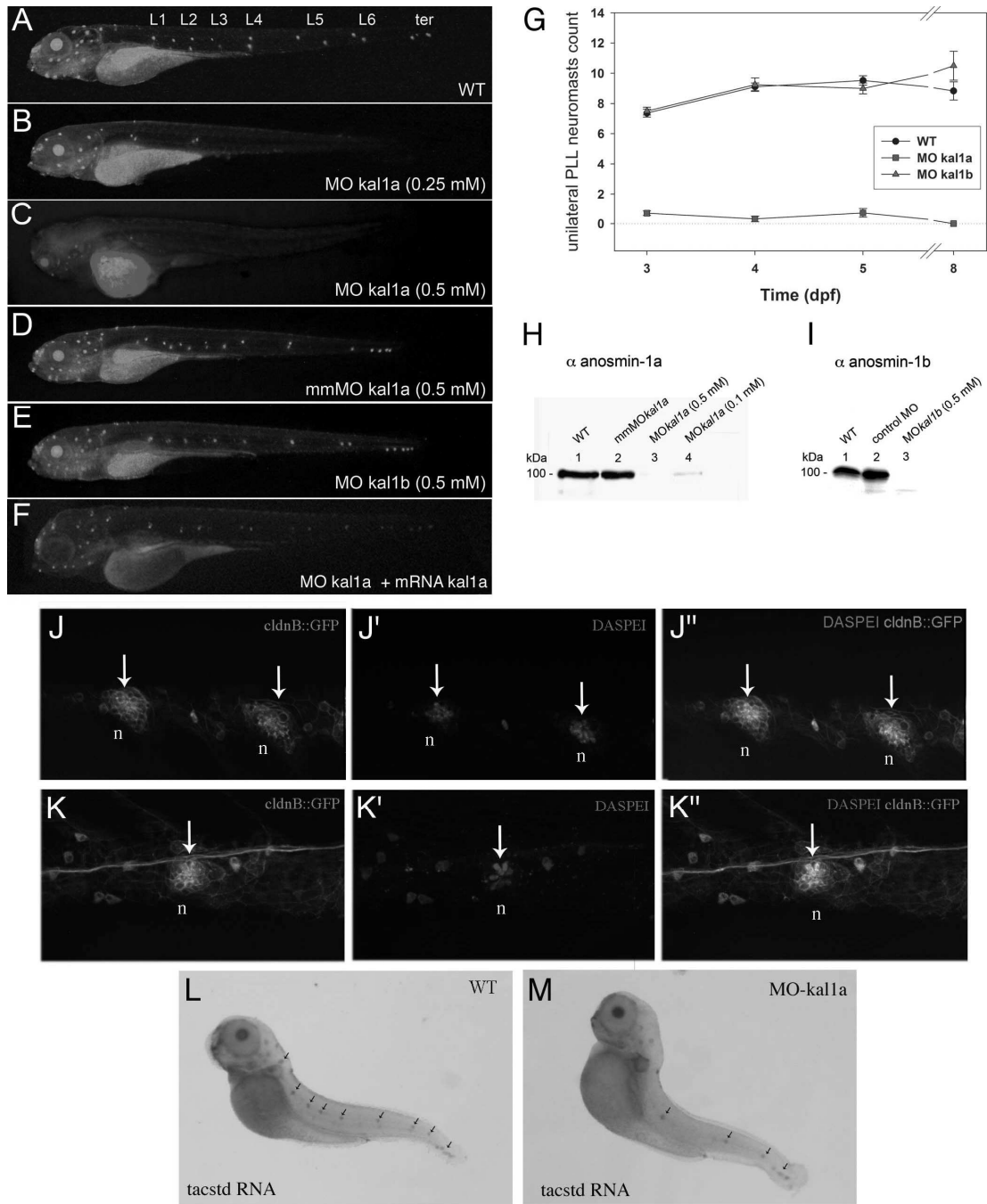


Figure2

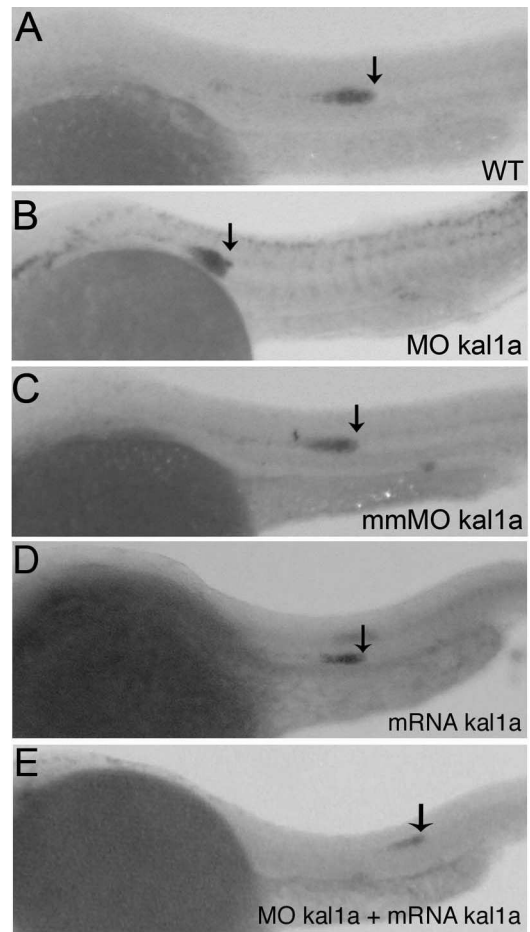


Figure 3

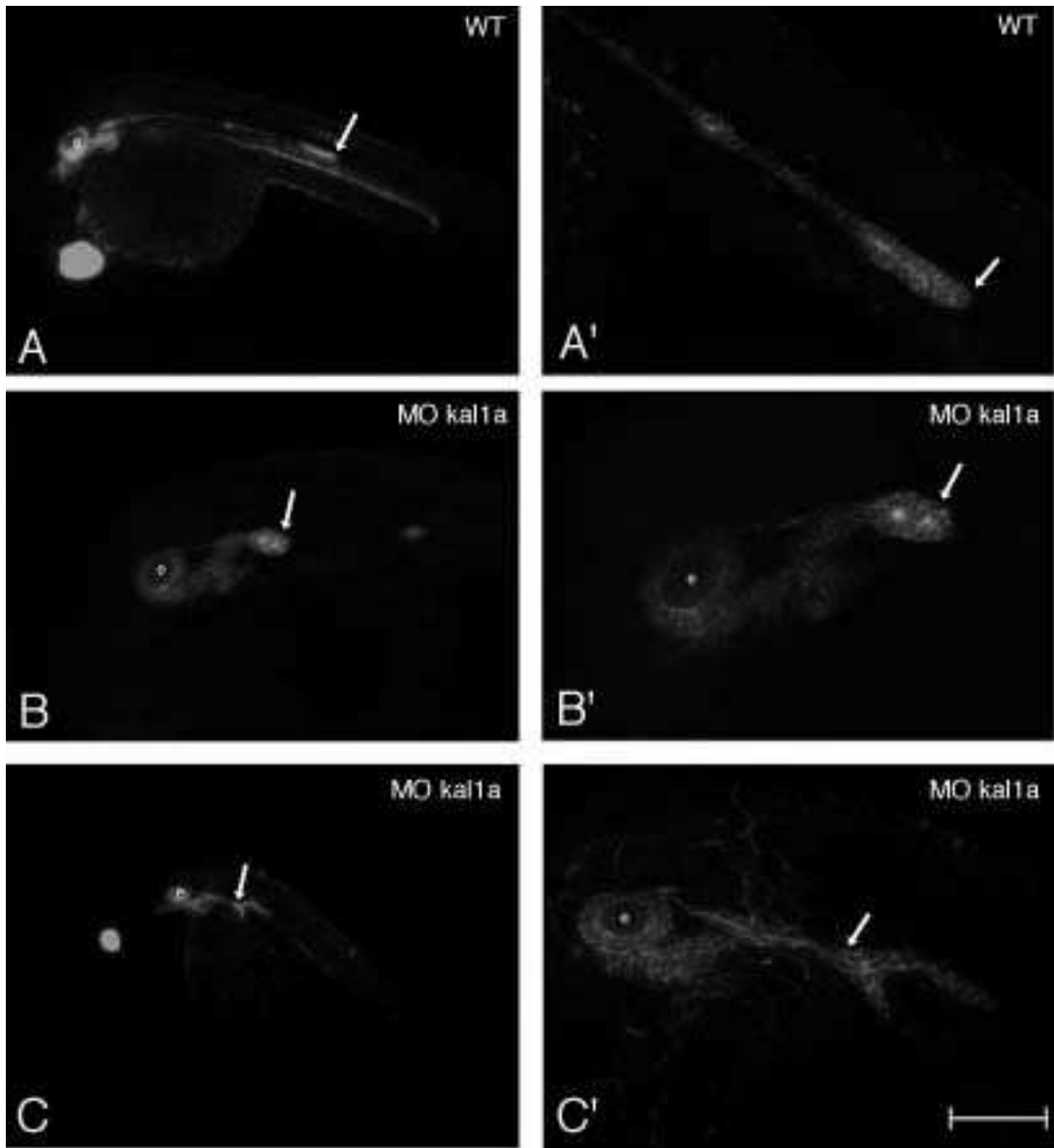


Figure 4

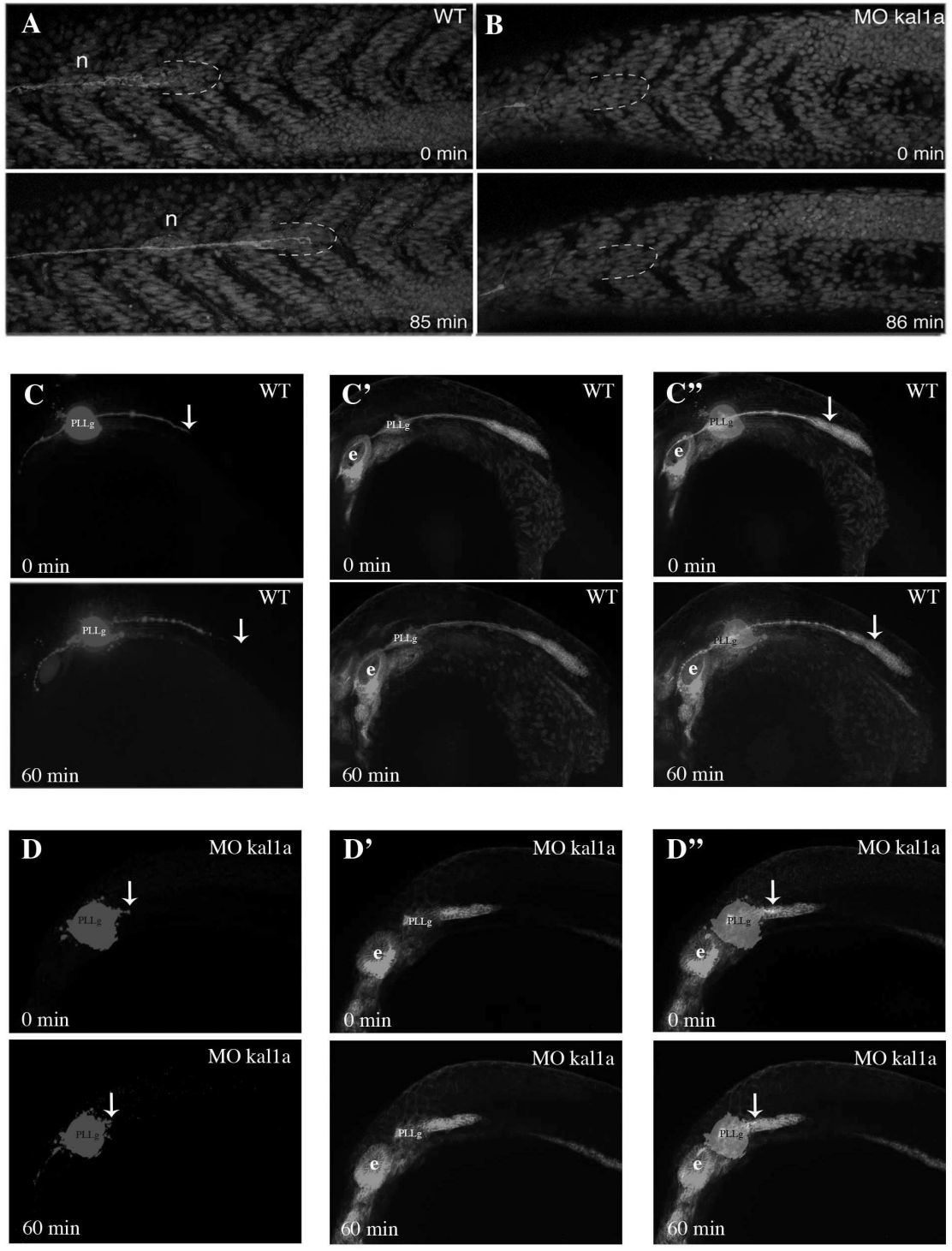


Figure 5

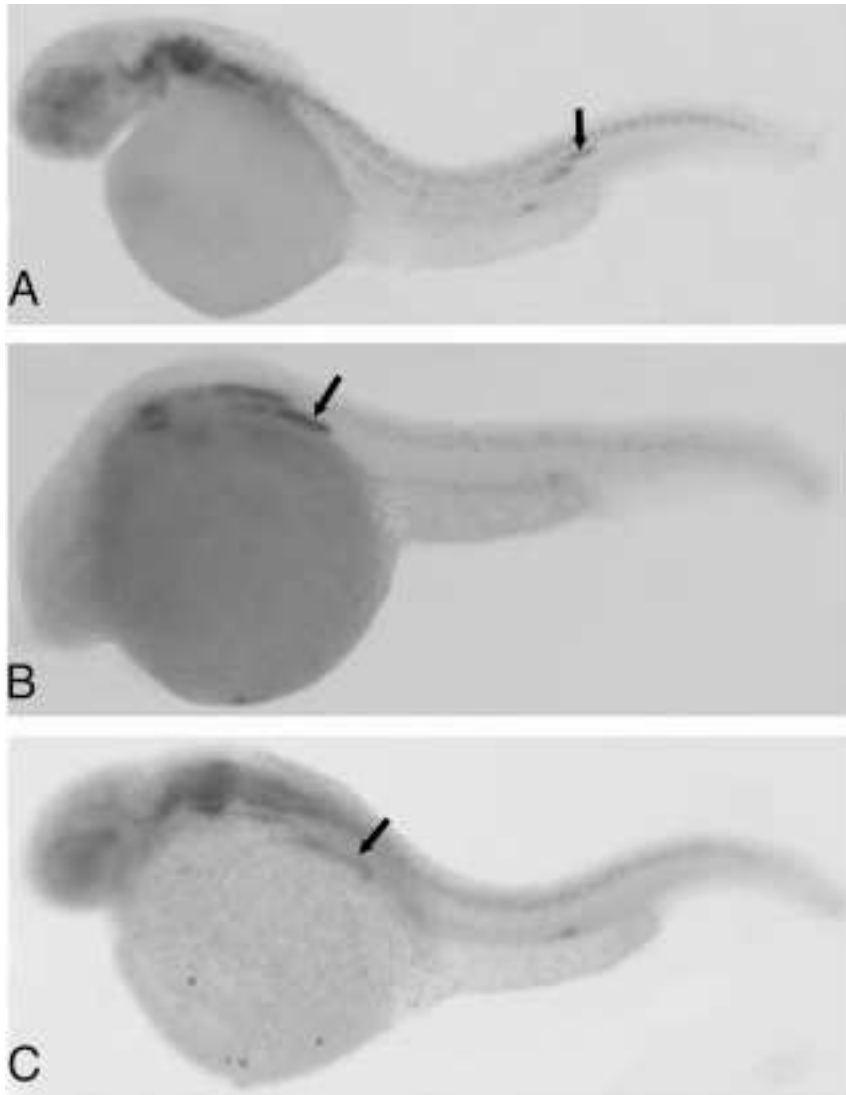


Figure 6

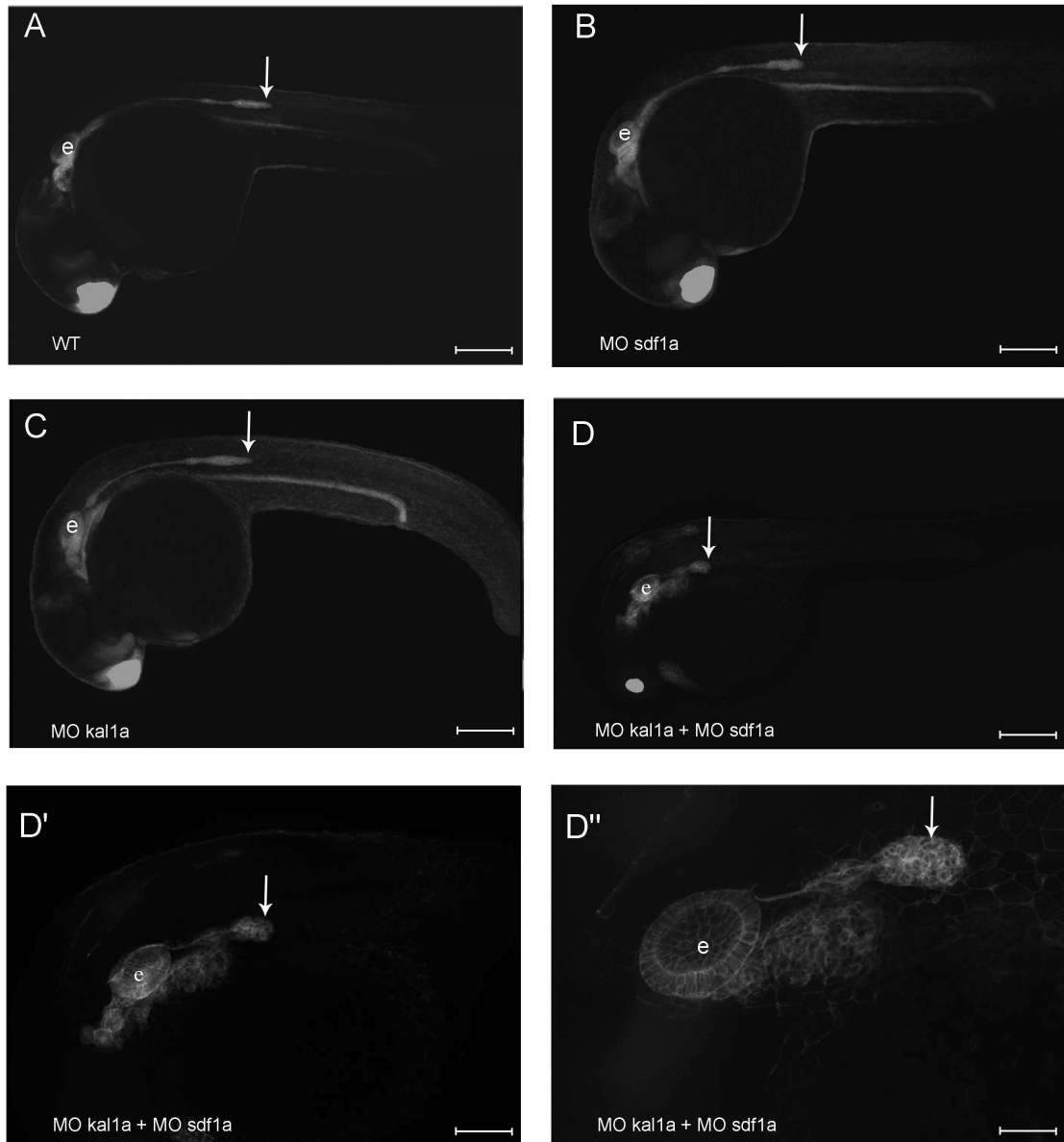


Figure 7

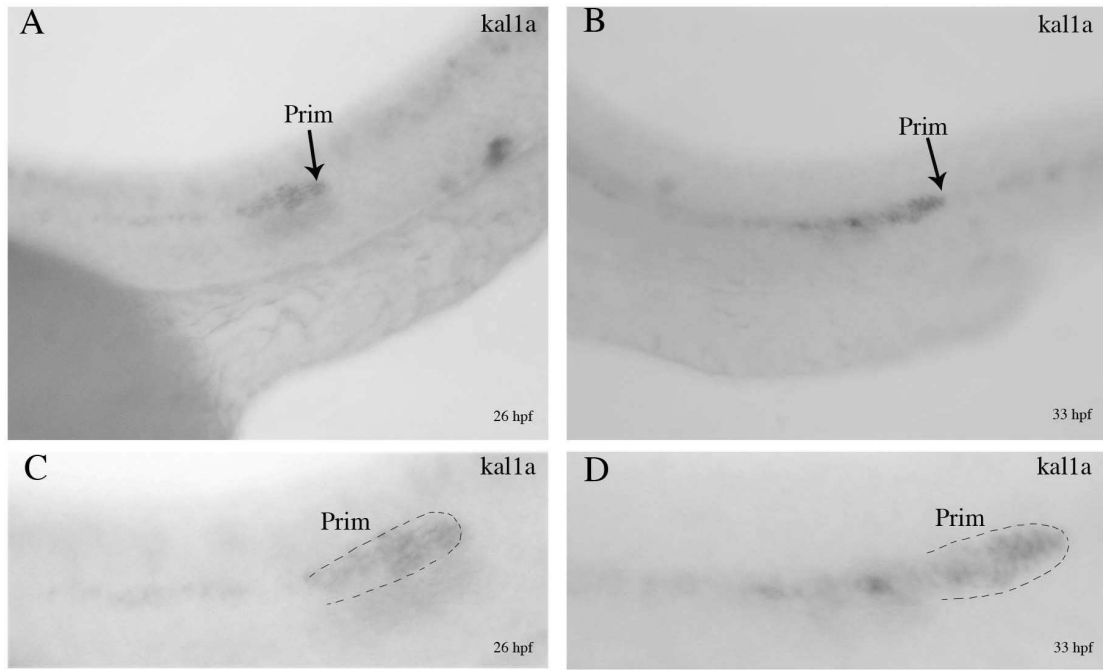


Figure S1

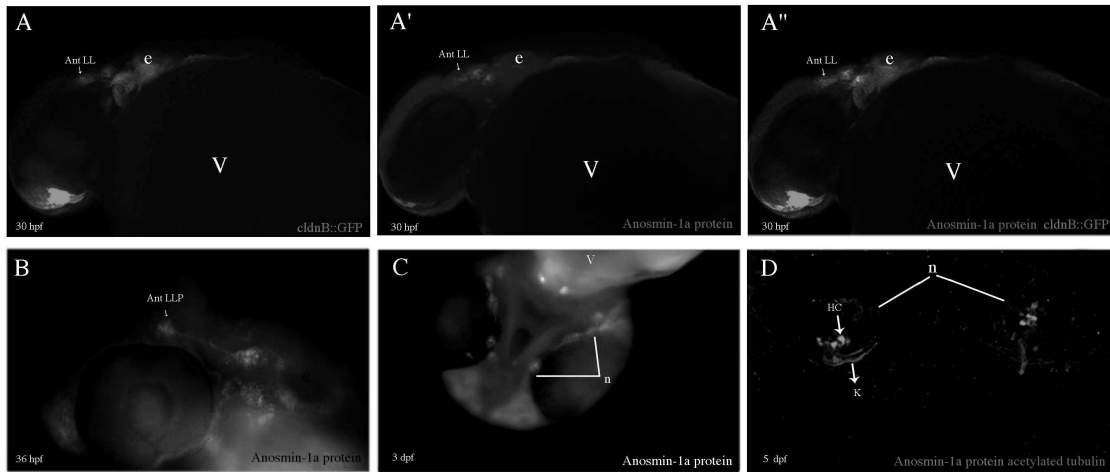


Figure S2

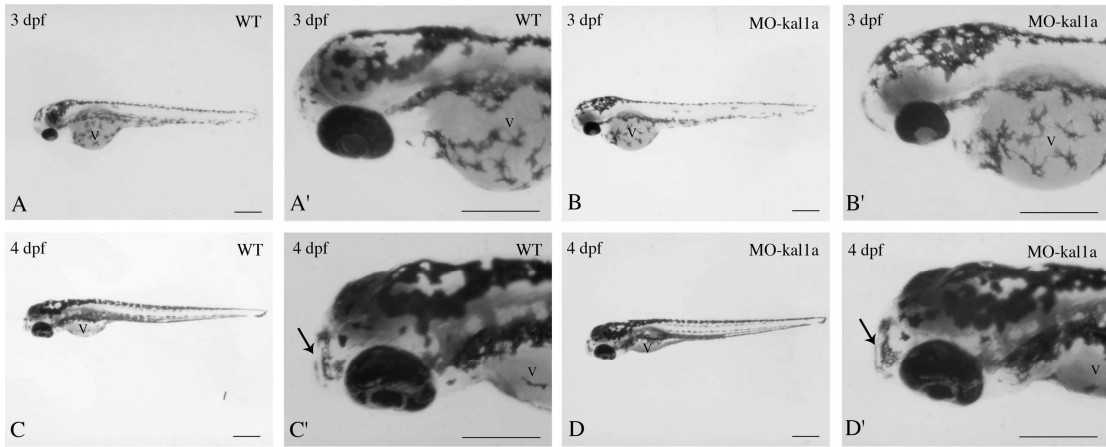


Figure S3

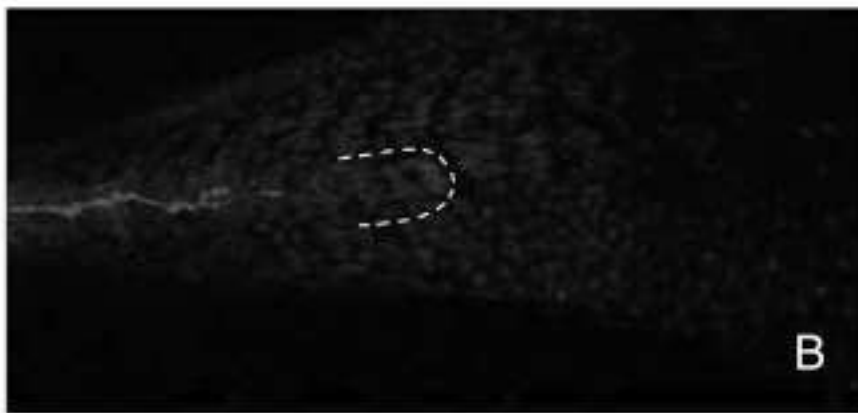
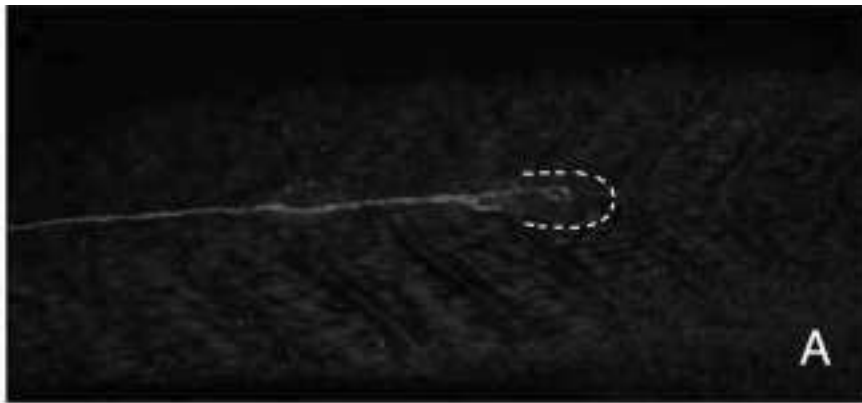


Figure S4

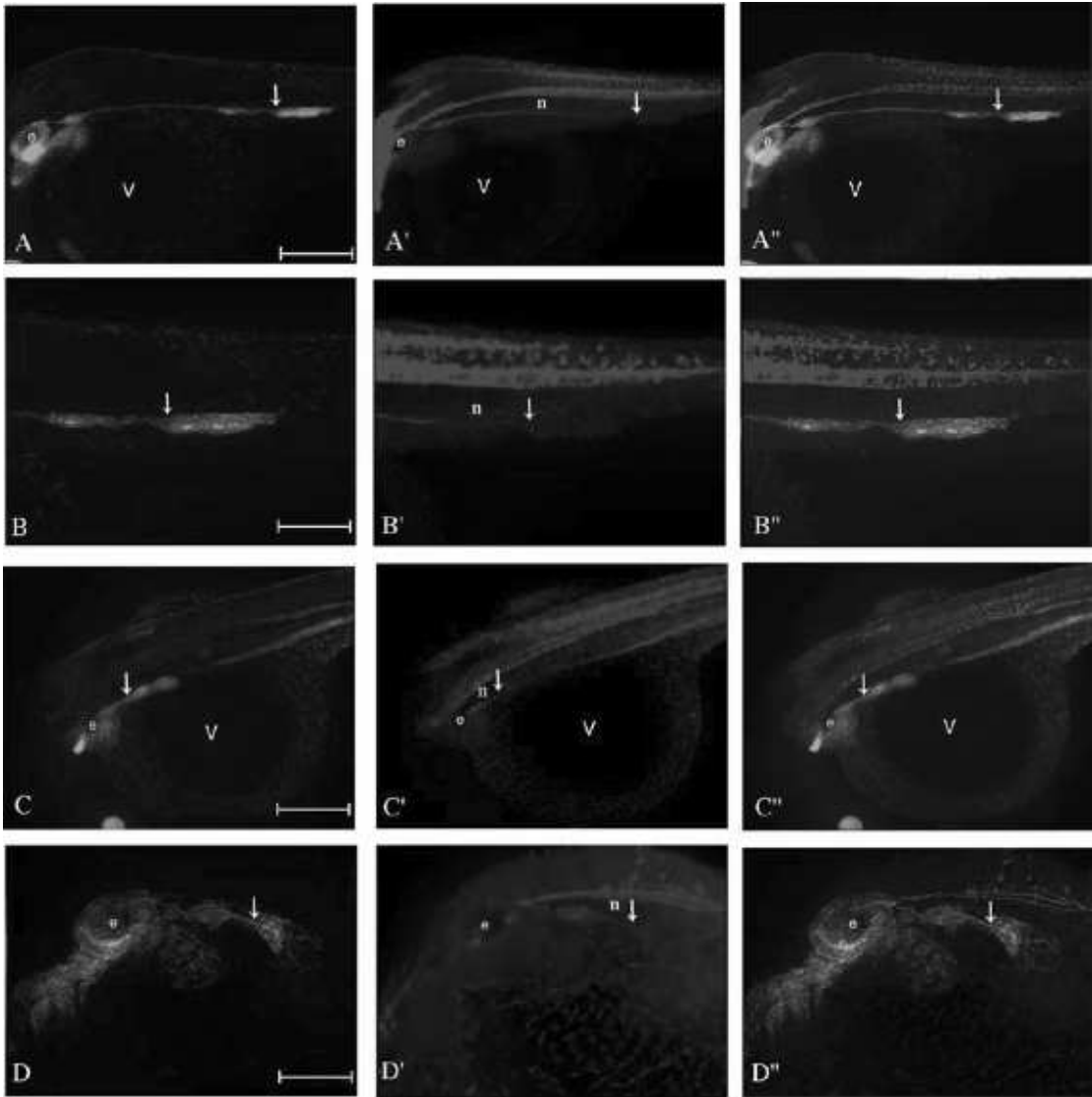


Figure S5

